A TRANSIENT MODEL FOR RADIANT HEATING AND COOLING TERMINAL HEAT EXCHANGERS APPLIED TO RADIANT FLOORS AND CEILING PANELS.

Dani Carbonell[1], Jordi Cadafalch[2] and Ricard Consul[2]

[1] RDmes S.L., Institut Politècnic Campus Terrassa (IPCT), Ctra. Nac. 150 km 14.6, 08227 Terrassa (Spain)

[2] Universitat Politècnica de Catalunya (UPC), Departament de Màquines i Motors Tèrmics (MMT), Institut Politècnic Campus Terrassa (IPCT), Ctra. Nac. 150 km 14.6, 08227 Terrassa (Spain)

1. Introduction

Radiant heating and cooling terminal heat exchangers have become very popular in the last decades because of the thermal comfort they provide and the energy savings potential respect to conventional systems.

Renewable energy technology's for heating and cooling such as solar, geothermal or both coupled, can be often optimized by the use of low/high impulse water temperature in winter/summer to the terminal heat exchangers. The radiant floors and ceilings are able to work efficiently with these conditions due to the large exchange area in both heating and cooling applications.

A careful design and optimal control strategy are important aspects to obtain expected energy savings (Abdelaziz, 2004). Therefore, a model capable to capture transient effects, system control strategies, and it's coupling with building energy simulation models, is of importance.

A transient numerical model for radiant floors and ceilings is presented and validated. The model has been implemented in RDmes online web platform (OTV) and can solve both steady and transient states for sizing and predicting respectively. The radiant floor/ceiling model has been developed under the frameworks of the IEA-Task44 (Solar and Heat Pump Systems) and FREDSOL project (Cadafalch, 2010).

2. Mathematical formulation

The model developed is based on the composite fin model for radiant floors described by Kilkis et al. (1994) coupled with a multi layer model as explained by Cadafalch (2009). The multi layer model solves the transient one-dimensional conduction of the different layers. The two models are coupled considering the heat flow from the pipe as a sink source term in a typical transient conduction problem (Patankar, 1980).

The model can be used for any terminal heat exchanger device with almost no significant modifications. The multi layer model can include any number of predefined-type layers which provides generality to the model. In fact, a similar approach has been used by Cadafalch (2009) to successfully model a flat plate collector. The model is applied in this study for radiant floors and ceilings and validated over a large set of cases.

2.1 The composite fin model

The fin is composed by several layers of different materials. The total heat transfer loss/gain U_L at the surface between the heat exchanger and the room air is calculated from the radiative (r) and convective (c) terms as:

$$U_L = U_r + U_c \quad \text{(eq. 1)}$$

In order to calculate the fin efficiency, it is necessary to define the total (T) conductivity of the composite fin with n covers:

$$\lambda_T = \frac{\sum_1^n \lambda_i x_i}{x_T} \quad \text{(eq. 2)}$$

where x_i is the thickness of the layer i and x_T is the total fin thickness. Special attention should be paid to the conductivity of the layer where the pipe is present. Jin et al. (2010a) proposed an expression to evaluate this equivalent conductivity based on a relation between a finite volume method and their simpler model:

$$\lambda_{eq} = 8.545 \ln(2.0335 + \lambda_p)(1.1596 + \lambda_{lp})(1.3219 + A_r)^{-1.4264} \quad \text{for } \lambda_p < 2W/mK \text{ (eq. 3)}$$

$$\lambda_{eq} = -0.031 + 23.8723(0.2844 + \lambda_{lp})(-0.9502 + A_r)^{-1.5753} \quad \text{for } \lambda_p \geq 2W/mK \text{ (eq. 4)}$$

Here the subscripts lp and p are used to refer to the layer where the pipe is embedded and the pipe respectively. The area ratio is defined by:

$$A_r = \frac{4MD_o}{\pi D_o^2} \text{(eq. 5)}$$

being D_o the external pipe diameter and M the distance between pipes.
The fin efficiency is defined by:

$$\eta = \frac{tanh(mL_f)}{mL_f} \quad \text{(eq. 6)}$$

where the fin length is obtained from:

$$L_f = \frac{M - D_o}{2} \quad \text{(eq. 7)}$$

and the parameter m as:

$$m = \sqrt{\frac{U_L}{\lambda_T x_T}} \quad \text{(eq. 8)}$$

At this step, it is useful to define the floor/ceiling efficiency F':

$$F' = \frac{1/U_L}{M[\dfrac{1}{U_L[D_o + (M - D_o)\eta]} + \dfrac{1}{h_i \pi D_i} + \dfrac{1}{C_b}]} \quad \text{(eq. 9)}$$

where h_i is the fluid to pipe heat transfer coefficient and C_b the bound conductance.

With the efficiency F', the fluid outlet temperature $T_{f,o}$ can be evaluated assuming an exponential distribution (Duffie and Beckman, 1991):

$$T_{f,o} = T_a + (T_{f,i} - T_a)e^{\frac{-U_L A_t F'}{\dot{m}_{in} c_p}} \quad \text{(eq. 10)}$$

being T_a the ambient temperature, $T_{f,i}$ the fluid inlet temperature, A_t the total floor/ceiling surface area, $\dot{m}_{in}$ the inlet mass flow and c_p the specific heat capacity.

The useful heat Q_u is then obtained from:

$$Q_u = \dot{m}_{in} c_p (T_{f,o} - T_{f,i}) \text{ (eq. 11)}$$

In order to obtain the average floor/ceiling surface temperature, the renovation factor F_R is used:

$$F_R = \frac{Q_u}{A_t U_L (T_a - T_{f,i})} \text{ (eq. 12)}$$

The average temperature of the layer where the pipe is present is defined by:

$$T_{lp} = T_{f,i} + \frac{Q_u}{A_t} \frac{1 - F_R}{U_L F_R} \text{ (eq. 13)}$$

and the fluid averaged temperature as:

$$T_{f,av} = T_{f,i} + \frac{Q_u}{A_t} \frac{1 - F''}{U_L F_R} \text{ (eq. 14)}$$

where

$$F'' = \frac{F_R}{F'} \text{ (eq. 15)}$$

2.2 Heat transfer coefficients

Several expressions have been developed for free and mixed convection heat transfer in horizontal plates both for heating and cooling applications. In the present model, the expressions from ASHRAE (2008) are used for cooled floor/ceiling, while for heated floor/ceiling, the equations are calculated as explained by Awbi et al. (1999). When mixed convection is present, the equations from Neiswanger et al. (1987) and Awbi et al. (2000) are employed. In order to calculate the heat transfer coefficients for radiation, the simplified model presented by Kilkis et al. (1994) is used.

2.3 The multi layer model

The model considers the transient one-dimensional heat transfer through N different layers with internal heat sources. Each layer is characterized by a heat transfer coefficient Λ_i in $[W / m^2 K]$, a thermal capacity c_i in $[J / m^2 K]$ and a heat source $\dot{q}_v$ in $[W / m^2]$ (Cadafalch, 2009). See Fig. 1 for details.

To identify each layer a subindex i is used from $i=1$ to $i=N$ corresponding to the bottom and top layers respectively. Linear temperature distribution in each layer is assumed. Therefore, the distribution of temperatures through all layers is a polyline with the vertexes at the interlayer surfaces.

Numerating the temperature of the different interlayer surfaces from 0 (bottom) to N (top), the temperature of limiting surfaces of the layer i are T_{i-1} and T_i.
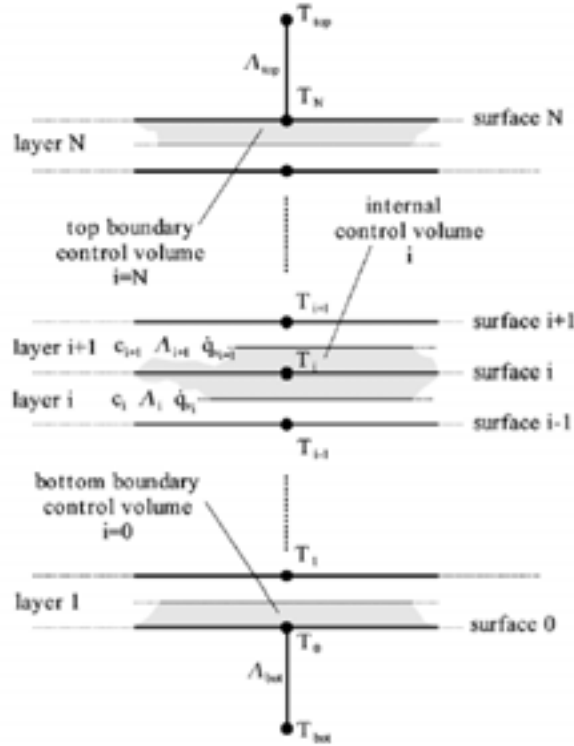
Fig. 1: Multi layer configuration

The temperature T_i at each interlayer surface is evaluated by solving the energy conservation law in a control volume made up by half of the two touching layers. The resulting discretized equation, using an implicit temporal discretization and a first order scheme for the time derivatives, reads as follows:

$$0.5(c_i + c_{i+1})\frac{T_i - T_i^0}{\Delta T} = 0.5(\dot{q}_{v,i} + (\dot{q}_{v,i+1}) + \Delta_i(T_{i-1} - T_i) - \Delta_{i+1}(T_i + T_{i+1}) \quad \text{(eq 16)}$$

where ΔT is the time increment and the superindex *0* refers to the value of the previous time step.

The bottom and top layers are related to the surroundings of the multilayer by means of a heat transfer coefficient and a surrounding (or ambient) temperature, Λ_{bot} and T_{bot} for the bottom, and Λ_{top} and T_{top} for the top.

Temperatures at the boundaries of the multilayer system, T_0 and T_N, are calculated by solving the energy conservation law in a control volume consisting of the external half of the layer and considering the appropriate boundary conditions. See the boundary control volumes indicated in Fig.1.

As a result, a set of *N+1* non-linear algebraic equations with the *N+1* unknown temperatures, are drawn. Non-linearity of the equations arises from possible temperature dependence of the parameters Λ_i, c_i and $\dot{q}_v$. An iterative solver based on a tridiagonal matrix algorithm is used to solve the resulting equation system (Patankar 1980).

By convention, the bottom layer of Fig.1 is the ground in a radiant floor and the top part of the roof in a radiant ceiling. Therefore, the temperature of the last surface T_{N+1} is always the average surface temperature of the floor/ceiling "*panel*" $T_{p,av}$.

The coupling between the multi layer and the fin composite models is due to the term $\dot{q}_v$ of the layer where the pipe is present:

$$\dot{q}_{v,lp} = -\frac{F'U_L}{1-F'}\left(T_{lp} - T_{f,av}\right) \text{ (eq 17)}$$

3. Results

The model has been validated under steady state conditions with a large set of experimental data in some cases of interest. Some of these results are shown hereafter. Comparison between the numerical model and the experimental data from other sources is presented. The validation in transient states has not been provided due to the lack of experimental data found in the literature useful for this purpose. This kind of validation will be provided in a near future work.

The first case analyzed is a radiant floor presented by Song, 2005. Results of interest for the present study are the average floor temperatures under heating and cooling conditions. This study was realized on a radiant floor composed by four layers: concrete, insulation, mortar with an embedded pipe and the floor covering. Several floor coverings were analyzed. Constructive details of the floor and thermal properties of each layer can be found in the source article (Song, 2005).
The experimental data were provided using several floor covering materials and different fluid inlet temperatures. The average floor temperatures of the numerical calculations and experiments (in parenthesis) are presented in Tab.1 for three different floor covering layers and six fluid inlet temperatures. The ambient temperatures of the room analyzed in the experiments were kept constant to 24ºC. Therefore the first two columns of Tab.1 are considered to be cooling cases, all the others are heating applications.

Tab. 1: Radiant floor numerical surface temperature $T_{p,av}$ compared to experimental data from Song, 2005 (in parenthesis)

$T_{f,i}\,[^0C]$ /Covering	15	20	25	30	35	40
Aluminum	16.79(-)	20.78(20.4)	24.78(24.8)	28.47(27.7)	32.00(31.2)	35.45(34.4)
Carpet	19.63(18.2)	22.03(20.5)	24.45(24.5)	26.41(26.0)	28.17(29.5)	29.83(29.7)
Plywood	18.36(19.1)	21.47(21.3)	24.59(23.5)	27.27(26.1)	29.75(28.1)	32.12(30.1)

As it can be observed from the results presented in Tab.1, the numerical results are quite accurate. Most of the errors are below 5% and the maximum differences are obtained in cooling cases and are always below 10%. The reason is that coefficients from the heating case may be more accurate, since they have been obtained from specific references for the present case.
The variations of the inlet fluid temperature and floor covering materials are captured properly by the model. However the mass flow rate effect has not been analyzed.

The next case has been selected in order to validate the model with different mass flow rates and also with different pipe conductivities. Experimental results of the radiant floor were presented by Jin et al. (2010b). The radiant floor is composed by seven layers (described from bottom to top): floor slab, insulation, cooling pipe, concrete, cement mortar, moisture proofing and wood layer. Details of the experiments can be found in the source article. Experimental data were presented using an average fluid temperature. The fluid inlet temperature in the numerical calculations has been adjusted until the average temperature was close to the experiments, even thought in the experiments this temperature was calculated assuming linear distribution. According to the experiments, the temperature at the bottom boundary is assumed to be 16.5ºC. In order to set the first temperature of the model T(0) to a predefined value, the heat transfer coefficient of the bottom boundary condition Λ_{bot} has been set to infinity along with the predefined temperature as T_{bot}.

Tab. 3: Radiant floor numerical results compared to experimental data from Jin et.al. , 2010b (in parenthesis)

$T_{f,av}$ [ºC]	$\dot{m}_{in}$ [kg/s]	$T_{p,av}$ [ºC]	Q_{cool} [W/m²]
10.87 (10.8)	0.134	20.68(20.7)	49.45
15.93(15.8)	0.134	22.72(22.4)	41.21
20.31(20.2)	0.134	23.55(23.8)	27.37
11.21(11.0)	0.0265	21.87(20.2)	51.16
11.03(11.4)	0.06615	21.39(19.9)	53.76
10.96(11.2)	0.1614	20.86(19.6)	50.99

Numerical calculations presented in Tab.3 are in the expected order of accuracy in all analyzed conditions. For the first three lines of Tab.3, the mass flow rate has been kept constant and the averaged fluid temperature has been modified. Results are very accurate in these three cases with errors below 2%. When the mass flow rate is modified, the errors increase slightly to values around 7-8%.

In the following study, the model has been used to simulate a radiant ceiling and compared to manufacturer's data from Jeong and Mumma (2004). In this case, the experimental data provided is the cooling capacity, Q_{cool}. Numerical results are presented in Tab.4 along with manufacturer's data (in parenthesis).

Experimental values were provided by Jeong et al. (2004) for panels of aluminium and steel, and inlet fluid temperatures ranging from 14ºC to 20ºC with 1ºC intervals. For the present comparison, the temperatures of 16 and 20ºC has been chosen for the two panels.

Tab. 4: Radiant ceiling numerical cooling capacity compared to experimental data from Jeong and Mumma, 2004 (in parenthesis)

Panel type	$T_{f,i}$ [ºC]	$T_{p,av}$ [ºC]	Q_{cool} [W/m²]
Aluminium	16	17.86	78.94(79.5)
Aluminium	20	21.07	46.09(43.9)
Steel	16	19.20	64.97(76.6)
Steel	20	21.88	38.25(42.5)

Results for aluminium panel match quite well manufacturer's data for both inlet fluid temperatures. However, numerical results in the case of steel panel are significantly lower than experimental data with errors around 15% and 10% for 16ºC and 20ºC fluid inlet temperature respectively. Notice that errors in aluminium panel are around 0.7% and 4.5% for 16ºC and 20ºC water inlet temperature respectively. Since the source article of Jeong and Mumma (2004) does not provide any additional information of the experiments and panel configuration details, it is difficult to give a reason for this difference when a steel panel is used. It may be possible that porosity in the ceiling panel or any other method for enhancing convection would be present in the real steel panel and may cause these differences. In fact, numerical results presented by Jeong and Mumma (2004) using the four different models they compared, were also more accurate for the aluminium panel.

In summary, the model performs quite well for radiant floors with several layers both in heating and cooling applications under steady state conditions. The model applied to radiant ceilings also predicts satisfactory results. However, more studies must be realized using a more detailed radiant ceiling experimental setup.

4. Conclusions

A generic transient model for terminal heat exchangers has been developed and applied to radiant floors and ceilings in heating and cooling applications. The model has been validated with comparisons against experimental data under steady state conditions. Transient states validation has not been provided due to the lack of experimental data found in the literature. The dynamic validation will be provided in near future works. The model can be applied to radiant floors and ceilings without any modification providing a quite general model.

The model has been shown to perform quite well under steady state conditions over a large number of cases. However, more validation studies are needed for ceilings panels using a well defined experimental setup.

5. Acknowledgements

6. References

Abdelaziz, L., 2004. Development of a radiant heating and cooling model for building energy simulation software. Building and Environment. 39, 421-431.

ASHRAE, 2008. Panel heating and cooling, in : HVAC Systems and equipment. American Society of Heating, Refrigerating and Air-Conditioning Engineers Inc, Atlanta, GA.

Awbi, H.B., Hatton, A., 1999. Natural convection from heated room surfaces.
Energy and Buildings. 30, 233-244.

Awbi, H.B., Hatton, A., 2000. Mixed convection from heated room surfaces.
Energy and Buildings. 32, 153-166.

Cadafalch, J., 2009. A detailed numerical model for flat plate solar thermal devices.
Solar Energy. 83, 2157-2164.

Cadafalch, J., Consul , R. , Carbonell, D., Levi, M., 2010. Air conditioning solar plant for a small office, located in the Mediterranean climate. Proceedings of EuroSun 2010, International Conference on Solar Heating, Cooling and Buildings, September-October 2010. Graz, Austria.

Duffie, J.A., Beckman, W.A., 1991. Solar engineering of thermal processes. John Wiley & Sons INC.

Jeong, J.W., Mumma, S.A., 2004. Simplified cooling capacity estimation model for top insulated metal ceiling radiant cooling panels. Applied Thermal Engineering. 24, 2055-2072.

Jin, X., Zhang, X., Luo, Y., 2010a. A calculation method for the floor surface temperature in radiant floor system. Energy and Buildings. 42, 1753-2552.

Jin, X., Zhang, X., Luo, Y., Cao, R., 2010b. Numerical simulation of radiant floor cooling system: The effects of thermal resistance of pipe and water velocity on the performance. Building and Environment. 45 2454-2552.

Neiswanger, L., Johnson, G.A., Carey, V.P., 1987. An experimental study of high Rayleigh number mixed convection in a rectangular enclosure with restricted inlet and outlet openings. Journal of Heat Transfer. 109, 446-453.

OTV RDmes Technical Virtual Office, www.rdmes.com

Patankar, S., 1980. Numerical heat transfer and fluid flow. Hemisphere Publishing Corporation.

Solar and Heat Pump Systems, Task44, Annex-38, Solar Heating and Cooling Programme, International Energy Agency.

Song, G-S., 2005. Buttock responses to contact with finishing materials over the ONDOL floor heating system in Korea. Energy and Buildings. 37, 65-75.

Kilkis, I.B., Sager, S.S., Uludag, M., 1994. A simplified model for radiant heating and cooling panels. Simulation Practice and Theory. 2, 61-76.